The ins and outs of ligand binding to CCR2

Zweemer, A.J.M.

Chapter 4

Discovery and mapping of an intracellular antagonist binding site at the chemokine receptor CCR2

Annelien J.M. Zweemer
Julia Bunnik
Margo Veenhuizen
Fabiana Miraglia
Eelke B. Lenselink
Maris Vilums
Henk de Vries
Arthur Gibert
Stefanie Thiele
Mette M. Rosenkilde
Adriaan P. IJzerman
Laura H. Heitman

Molecular Pharmacology ***2014*** *86(4):358-368*

Abstract

The chemokine receptor CCR2 is a G protein-coupled receptor that is involved in many diseases characterized by chronic inflammation, and therefore a large variety of CCR2 small molecule antagonists has been developed. On the basis of their chemical structures these antagonists can be roughly divided into two groups with most likely two topographically distinct binding sites. The aim of the current study was to identify the binding site of one such group of ligands, exemplified by three allosteric antagonists, CCR2-RA-[R], JNJ-27141491 and SD-24.

We first used a chimeric CCR2/CCR5 receptor approach to obtain insight into the binding site of the allosteric antagonists, and additionally introduced eight single point mutations in CCR2 to further characterize the putative binding pocket. All constructs were studied in radioligand binding as well as functional IP turnover assays, providing evidence for an intracellular binding site for CCR2-RA-[R], JNJ-27141491 and SD-24. The most important residues for binding were found to be the highly conserved tyrosine $Y^{7.53}$ and phenylalanine $F^{8.50}$ of the $NPxxYX_{(5,6)}F$ motif, as well as $V^{6.36}$ at the bottom of TM-VI and $K^{8.49}$ in helix-VIII. In addition, we found two other residues at locations surrounding this binding pocket, which differently affected the three allosteric ligands.

These findings demonstrate for the first time the presence of an allosteric intracellular binding site for CCR2 antagonists. This contributes to an increased understanding of the interactions of diverse ligands at CCR2 and may allow a more rational design of future allosteric antagonists.

Introduction

The chemokine receptor CCR2 is a G protein-coupled receptor (GPCR) that is expressed on monocytes, dendritic cells, activated T lymphocytes and basophils, and therefore it plays an important role in the immune system [1-3]. These immune cells migrate towards increasing concentrations of chemokines at sites of inflammation as part of the immune response, also known as chemotaxis. CCR2 is activated by multiple chemokines, including CCL2, CCL7, CCL8, CCL11, CCL13 and CCL16. Besides its important role in physiology, increased levels of CCR2 and its ligands can induce severe tissue damage. This results in a large variety of diseases that are characterized by chronic inflammation [4-7], which makes CCR2 an attractive drug target for the pharmaceutical industry. As a consequence many CCR2 small molecule antagonists have been developed over the years, but unfortunately all clinical candidates tested so far appeared to lack efficacy in man.

Most small molecule chemokine receptor antagonists bind at the main binding pocket in the upper half (exterior part) of the transmembrane (TM) helices, usually with one part in the so-called major binding pocket (surrounded by TM helices III, IV, V, VI and VII) and the other part in the minor binding pocket (surrounded by TM helices I, II, III and VII) [8]. Many small molecule antagonists contain a positively charged basic nitrogen that interacts with the conserved negatively charged glutamic acid residue (E291$^{7.39}$) in TM-VII, which is directly located in between the major and minor binding pocket [9]. An example of such a CCR2 antagonist is INCB3344 (Fig. 1), to which we refer as an orthosteric antagonist, since it was previously reported to inhibit CCR2 in a competitive manner with respect to the chemokine ligand CCL2 [10, 11]. Interestingly, other classes of antagonists were discovered to bind at a different binding site than INCB3344 [10]. It was shown that these antagonists, CCR2-RA-[R] and JNJ-27141491 (Fig. 1), possess structural features different from the orthosteric antagonists and inhibit CCR2 in a noncompetitive manner with respect to CCL2. The current study took these findings as the starting point to resolve the location of the binding site for these allosteric CCR2 antagonists. For several other chemokine receptors the presence of an allosteric binding site has been reported [12, 13]. Some of these antagonists bind exclusively to the major or minor binding pocket [14] and their binding site can even be directed towards the extracellular loops, as illustrated in the CXCR4 crystal structure for the small molecule antagonist IT1t [15]. In addition, an allosteric binding site on the intracellular side of the receptor in the C-terminal domain has been suggested for the chemokine receptors CXCR2, CCR4 and CCR5 [16-18].

In the present study we first showed that a previously described antagonist with a sulfonamide scaffold (SD-24) is also an allosteric antagonist (Fig. 1) [19]. Subsequently, we used a CCR2/CCR5 chimeric approach to get insight into the binding site of allosteric antagonists for CCR2 and made single point mutations in CCR2 to further map this binding pocket. We discovered the existence of an intracellular binding site in CCR2 that is recognized by (at least) three chemically different classes of antagonists. Finally, we discuss the compounds' mechanism of action and the implications for targeting CCR2 in disease states.

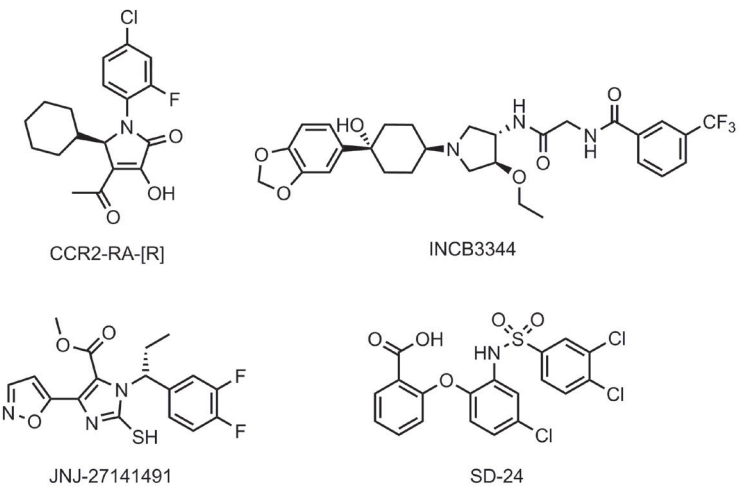

Fig. 1. Chemical structures of the orthosteric CCR2 antagonist INCB3344 and the allosteric CCR2 antagonists CCR2-RA-[R], JNJ-27141491 and SD-24.

Materials and Methods

Chemicals and reagents. CCL2 was purchased from PeproTech (Rocky Hill, NJ). INCB3344, JNJ-27141491 and CCR2-RA-[R] were synthesized according to published methods [47-50]. SD-24 (sulfonamide derivative #24 from the Peace et al. paper) was synthesized in-house, according to procedures described previously [19]. [^{3}H]-INCB3344 (specific activity 32 Ci mmol^{-1}) and [^{3}H]-CCR2-RA (specific activity 63 Ci mmol^{-1}) were custom-labeled by Vitrax (Placentia, CA). ^{125}I-CCL2 (2200 Ci/mmol), ^{125}I-CCL3 (2200 Ci/mmol), [^{35}S]GTPγS (1250 Ci/mmol) and *myo*-[^{3}H] inositol (PT6-271) (94.5 Ci/mmol) were purchased from Perkin-Elmer (Waltham, MA, USA). Bovine serum albumin (BSA, fraction V) was purchased from Sigma (St. Louis, MO, USA). Bicinchoninic acid (BCA) and BCA protein assay reagent were obtained from Pierce Chemical Company (Rockford, IL, USA). Polyethyleneimine (PEI) was obtained from Polysciences Inc.

(Warrington, PA, USA). Wild-type (WT) FLAG-tagged CCR5 was cloned in-house from a leukocyte cDNA library, while WT FLAG-tagged CCR2 cDNA was kindly provided by Dr Tim Wells (GlaxoSmithKline, UK). The chimeric receptor CCR5-CCR2$_{all}$, was previously described [20], whereas CCR2-CCR5$_{C\text{-}term}$ and CCR5-CCR2$_{C\text{-}term}$ were designed in-house and cloned using PCR overlap extension technique (Piscataway, NJ). pcDNA3.1+ plasmid containing the WT CCR2 with a 3x hemagglutinin (HA) epitope tag at the N-terminus was kindly provided by James Pease (Imperial College London, UK). The promiscuous G protein G$\alpha_{\Delta 6qi4myr}$ (G$_{qi4myr}$) was kindly provided by Evi Kostenis (University of Bonn, Germany). Tango CCR2-bla U2OS cells stably expressing human CCR2 (U2OS-CCR2) were obtained from Invitrogen (Carlsbad, CA). CHO (Chinese hamster ovary) cells were obtained from Hans den Dulk (Leiden University, the Netherlands) and COS-7 cells were obtained from ATCC (Rockville, MD). The monoclonal rabbit anti-HA-tag antibody and the HRP-conjugated goat anti-rabbit antibody were obtained from Novus Biologicals (Cambridge UK). The monoclonal mouse anti-FLAG M1 antibody was obtained from Sigma (St. Louis, MO) and the HRP-conjugated goat anti-mouse antibody was obtained from Pierce (Rockford, IL). AG 1-X8 anion exchange resin was obtained from Bio-Rad (Hercules, CA). All other chemicals were obtained from standard commercial sources.

Site-directed mutagenesis. pcDNA3.1+ plasmids containing the human CCR2 mutants I208A$^{5.45}$ and E291A$^{7.39}$ (superscript indicates the Ballesteros Weinstein numbering system [21], in which transmembrane residues are assigned two numbers that belong to the helix number and the residue number relative to the most conserved residue in this helix, which is assigned 50) with a 3x hemagglutinin (HA) epitope tag at the N-terminus were kindly provided by James Pease (Hall et al., 2009). All other point mutations were generated by site-directed mutagenesis, using WT HA-tagged CCR2 plasmid DNA as a template for the generation of mutant plasmids by polymerase chain reaction (PCR) using the QuickChange® II Site-directed mutagenesis kit (Stratagene, the Netherlands) and the appropriate oligonucleotide primers (Eurogentec, the Netherlands), under conditions recommended by the manufacturer. All mutants were verified by DNA sequencing before use (LGTC, Leiden University, the Netherlands).

Cell culture. COS-7 cells and U2OS-CCR2 cells were cultured as described before [10, 20]. Chinese hamster ovary (CHO) cells were cultured in Ham's F12 culture medium supplemented with 10% (v/v) newborn calf serum, penicillin (50 IU/mL) and streptomycin (50µg/mL) at 37°C and 5% CO_2. Cells were subcultured twice weekly at a ratio of 1:20 by trypsinization on 10-cm ø plates.

Transfections. Transfections of COS-7 cells with FLAG-tagged CCR2, CCR5 or chimeric receptor were performed by the calcium phosphate precipitation method as described before [22]. Transfections of CHO cells with FLAG-tagged CCR2, CCR5 or chimeric receptor, as well as HA-tagged WT or mutant CCR2, were performed with polyethyleneimine (PEI). For this purpose, CHO cells were grown to 50-60% confluence on 15-cm ø plates and transfected with 10 µg of plasmid DNA per 15-cm ø plate. Briefly, 10 µg of plasmid DNA was diluted in a sterile 150 mM NaCl solution and subsequently mixed with PEI solution (1mg/mL) to obtain a DNA:PEI mass ratio of 1:6. The mixture was incubated for 20 min at room temperature before transfection. The culture medium of the cells was refreshed and 1 mL of DNA/PEI mixture was added to cells and incubated for 48 hrs at 37°C and 5% CO_2.

Cell membrane preparation. Membranes were prepared as described before [10]. Briefly, cells were scraped from 15-cm ø plates upon which the membranes and cytosolic fractions were separated during several centrifugation steps. Finally, the membrane pellet was resuspended in ice-cold 50 mM Tris-HCl buffer containing 5 mM $MgCl_2$, pH 7.4, and aliquots were stored at −80 °C. Membrane protein concentrations were measured using a BCA protein determination with BSA as a standard [23].

Cell surface expression by Enzyme-Linked Immunosorbent Assay (ELISA). For transfections with WT and mutant CCR2 receptors containing a HA-tag, CHO cells were plated 24 hrs after transfection at a density of $1x10^6$ cells per well in a 96-well plate and incubated at 37 ºC and 5% CO_2 for 24 hrs. Cells were washed with PBS and incubated with rabbit anti-HA primary antibody (dilution 1:5000 in DMEM) for 30 min at RT. After a subsequent wash with DMEM/HEPES (25 mM), cells were incubated with HRP-conjugated goat anti-rabbit secondary antibody (dilution 1:5000 in DMEM) for 30 min at RT. The cells were washed twice with pre-warmed PBS, after which tetramethyl benzene (TMB) was added for 5 min in the dark at RT. The reaction was stopped by addition of 1 M H_3PO_4 and after 5 min absorbance was measured at 450 nm with a Victor^{2}V plate reader (Perkin Elmer, Waltham, MA, USA).

^{125}I-CCL2 binding assays. ^{125}I-CCL2 and ^{125}I-CCL3 whole cell binding assays on COS-7 cells transfected with WT FLAG-tagged CCR2, CCR5 or chimeric receptor were performed as described before [20]. In these assays ^{125}I-CCL2 was used for CCR2 and the two chimers CCR5-CCR2(all) and CCR2-CCR5(C-term), whereas ^{125}I-CCL3 was used for CCR5 and the chimer CCR5-CCR2(C-term). ^{125}I-CCL2 binding assays on U2OS-CCR2 cell membranes were performed as described before [10]. Briefly, the assay was performed in a 100 µL reaction

volume containing 50 mM Tris-HCl buffer (pH 7.4), 5 mM $MgCl_2$, 0.1% 3-((3-cholamidopropyl)-dimethylammonio)-1-propanesulfonate (CHAPS) and 15 µg of U2OS-CCR2 cell membrane protein at 37 °C. Displacement assays were performed with 0.1 nM ^{125}I-CCL2 using six concentrations of competing ligand for 150 min of incubation. At this concentration, total radioligand binding did not exceed 10% of the amount added to prevent ligand depletion. Non-specific binding was determined with 10 µM INCB3344. Reactions were terminated as described before.

[^{3}H]-INCB3344 binding assays. [^{3}H]-INCB3344 membrane binding assays were performed as described before [10]. For the FLAG-tagged CCR2, CCR5 and the chimera's expressed in CHO cells, homologous displacement studies were carried out with 2.1 nM and 5.0 nM [^{3}H]-INCB3344 to be able to determine the equilibrium dissociation constant K_D. Studies with HA-tagged WT and mutant receptors of CCR2 were carried out with a single concentration of 5.7 nM [^{3}H]-INCB3344. In all cases, eight concentrations of competing ligand were incubated for 120 min at 25 °C. Non-specific binding for mutant and WT CCR2 receptors was determined in the presence of 10 µM INCB3344. For the WT receptor the measured non-specific binding was equal to the experiments in which 10 µM BMS22 was used, as described in our previous study [10]. In all experiments, total radioligand binding did not exceed 10% of the amount added to prevent ligand depletion.

[^{3}H]-CCR2-RA binding assays. [^{3}H]-CCR2-RA membrane binding assay conditions were similar as those for [^{3}H]-INCB3344 binding assays as described before [10]. For the FLAG-tagged CCR2, CCR5 and the chimera's expressed in CHO cells, homologous displacement studies were carried out with 4.5 nM and 7.9 nM [^{3}H]-CCR2-RA to be able to determine the equilibrium dissociation constant K_D. Displacement assays with HA-tagged WT and mutant receptors of CCR2 were carried out with a single concentration of 7.9 nM [^{3}H]-CCR2-RA. In all cases, eight concentrations of competing ligand were incubated for 120 min at 25ºC. Non-specific binding was determined in the presence of 10 µM CCR2-RA-[R]. For the WT receptor the measured non-specific binding was equal to the experiments in which 10 µM JNJ-27141491 was used, as described in our previous study [10]. In all experiments, total radioligand binding did not exceed 10% of the amount added to prevent ligand depletion.

Inositol Phosphate turnover (IP Turnover) assay. IP turnover was measured in COS-7 cells co-transfected with WT FLAG-tagged CCR2, CCR5 or chimeric receptor and the promiscuous G protein G_{qi4myr}, as described before [20].

[^{35}S]GTPγS binding assay. The [^{35}S]GTPγS assay was performed as described before [10]. To determine G protein activation of the wild-type and mutant CCR2 receptors, 10 µg of CHO cell membranes were pre-incubated with 100 nM CCL2 (single point) or six increasing concentrations of CCL2 for 30 min at 25 °C. Then [^{35}S]GTPγS (0.3 nM) was added, after which the mixture was incubated for 90 min and samples were harvested as described before.

Data analysis. All experiments were analyzed using the non-linear regression curve fitting program Prism 5 (GraphPad, San Diego, CA, U.S.A.). pK_D values for the FLAG-tagged CCR2, CCR5 and chimeric receptors were calculated using the homologous competitive binding curve fit. The pIC_{50} values for WT and mutant CCR2 of INCB3344, CCR2-RA-[R], JNJ-27141491 and SD-24 were obtained by non-linear regression analysis of the displacement curves. Statistical analysis was performed with a two-tailed unpaired Student's *t*-test. All values obtained are means of at least three independent experiments performed in duplicate, unless stated otherwise.

Antagonist superposition, homology modeling and ligand docking. To best superimpose the three different antagonists, multiple ligand conformations of each individual compound were generated using MacroModel version 10.1 [24], with mixed torsional/low-mode sampling and default settings. Subsequently the different ligand conformations were aligned using the flexible ligand alignment method within Maestro [25] and selected based on their pose and shape similarity. A homology model of the chemokine CCR2 receptor was constructed using the homology modeling tool within Maestro [25-27]. This model was based on the structure of the chemokine CCR5 receptor co-crystalized with maraviroc (Protein Data Bank: 4MBS). The best model was selected based on the energy-based scoring function, while the sequence alignment between CCR2 and CCR5 was performed using ClustalW as implemented within Maestro. CCR2-RA-[R] was docked into the receptor homology model using the induced fit docking protocol [28, 29]. The grid center was placed based on residues D78$^{2.40}$, Y305$^{7.53}$, K311$^{8.49}$ and F312$^{8.50}$ with an automatic box size. Visualizations were created using PyMOL version 1.5.0.4. [30].

Results

Effect of sulfonamide SD-24 on CCR2 radioligand binding. The sulfonamide derivative SD-24 partially inhibited binding of ^{125}I-CCL2 to CCR2-expressing U2OS cell membranes to 27 ± 6 % at 10 µM, with a pIC_{50} of 7.2 ± 0.2 (Fig. 2). [^{3}H]-CCR2-RA was fully displaced with a pK_i value of 9.0 ± 0.1. On the contrary, SD-24 slightly increased [^{3}H]-INCB3344 binding to a maximum of 120 % at 1 µM SD-24, indicating it binds at a site different from the previously described [10, 11] orthosteric binding pocket of INCB3344 (Fig. 2).

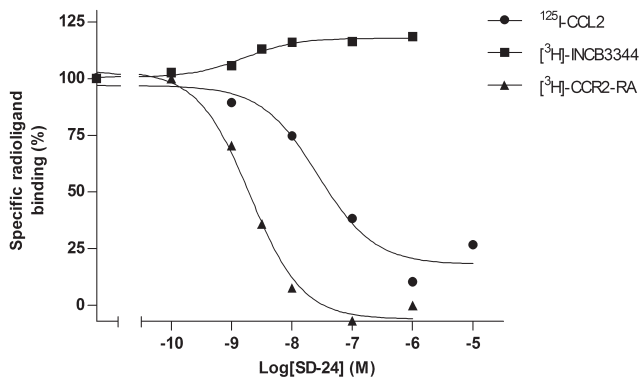

Fig. 2. Modulation of ^{125}I-CCL2, [^{3}H]-INCB3344 and [^{3}H]-CCR2-RA binding to U2OS cell membranes stably expressing CCR2 by increasing concentrations of the CCR2 antagonist SD-24. Results are presented as percentage of bound radioligand for one representative experiment performed in duplicate. SD-24 inhibited binding of ^{125}I-CCL2 with a pIC_{50} of 7.2 ± 0.2 and [^{3}H]-CCR2-RA with a pK_i of 9.0 ± 0.1. For ^{125}I-CCL2, 27 ± 6 % radioligand remained bound in the presence of 10 µM SD-24.

Comparison of CCR2 and CCR5. In order to identify regions that are responsible for binding of SD-24 and the other allosteric antagonists we compared the affinity of CCR2-RA-[R], JNJ-27141491 and SD-24 for CCR2 and its close homolog CCR5 (Fig. 3A) in whole cell radioligand binding assays using ^{125}I-CCL2 and ^{125}I-CCL3, respectively. CCR2-RA-[R] and JNJ-27141491 displaced ^{125}I-CCL2 from CCR2 with pIC_{50} values of 6.1 ± 0.1 and 6.6 ± 0.1, respectively (Table 1). In addition, JNJ-27141491 inhibited ^{125}I-CCL3 from binding to CCR5 with a pIC_{50} value of 5.4 ± 0.1, whereas CCR2-RA-[R] did not sufficiently displace ^{125}I-CCL3 from CCR5 to be able to determine its affinity for CCR5. The affinity of SD-24 for CCR2 could not be measured in this whole cell binding assay, and neither was any displacement of ^{125}I-CCL3 from CCR5 observed in the presence of SD-24 (Table 1). Differently, in the functional IP turnover assay the pIC_{50} values for CCR2 and CCR5 inhibition could be determined for all antagonists (Table 2). In this assay CCR2-RA-[R], JNJ-27141491 and SD-24 showed a 7-fold, 14-fold and 22-fold reduced potency to inhibit CCR5 compared to CCR2, respectively.

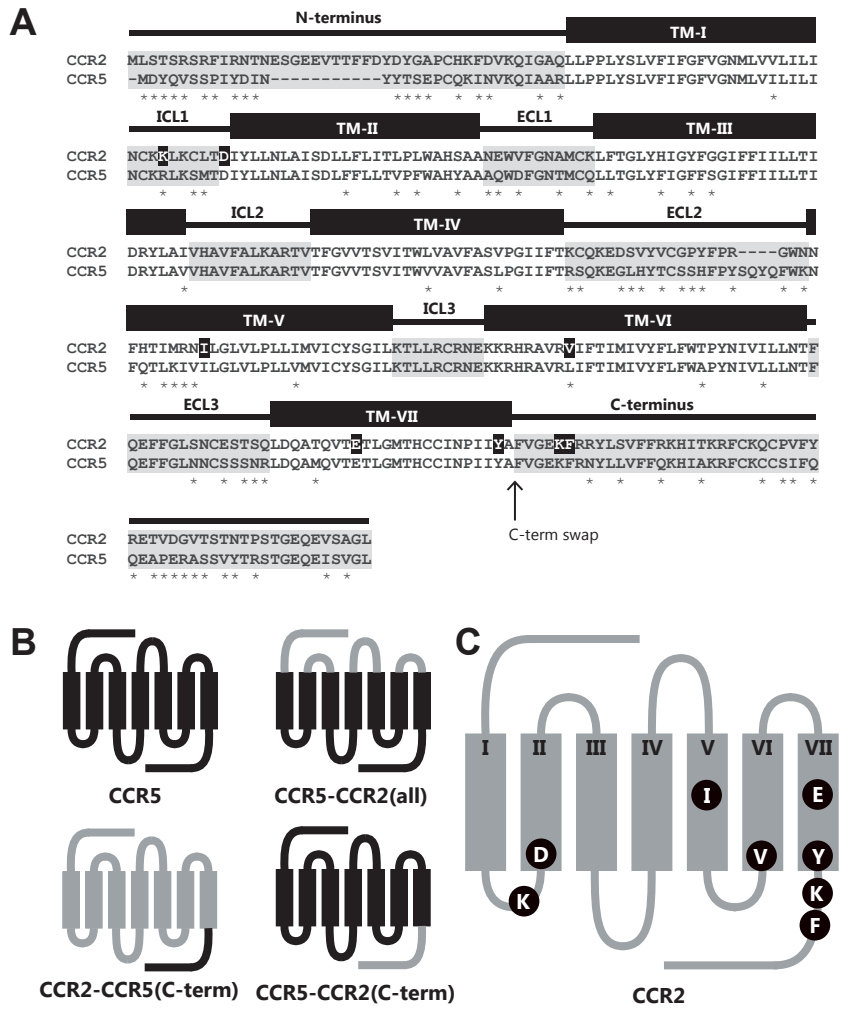

Fig. 3. (A) Sequence alignment with ClustalW2 of CCR2 and CCR5, for which the transmembrane regions as well as the intracellular and extracellular loops are indicated (bottom). Differing residues are indicated with an asterisk, and CCR2 residues mutated in this study are indicated in black. The arrow presents the location where the C-termini were swapped. The locations where the extracellular loops of CCR2 were inserted into CCR5 can be found in Thiele *et al.* 2011. (B) Schematic representation of CCR5 and the chimeric receptors CCR5-CCR2(all), CCR2-CCR5(C-term) and CCR5-CCR2(C-term). (C) Schematic representation of CCR2. The approximate location of the residues $K^{2.34}$, $D^{2.40}$, $I^{5.45}$, $V^{6.36}$, $E^{7.39}$, $Y^{7.53}$, $K^{8.49}$ and $F^{8.50}$ is indicated.

Table 1. Inhibition of chemokine whole cell binding by the endogenous chemokines or small molecule antagonists, for CCR2, CCR5 and the chimeric receptors expressed in COS-7 cells. The chemokine radioligand that was used for each construct is indicated in the first column.

	endogenous ligands (CCL2 or CCL3)		orthosteric INCB3344		allosteric CCR2-RA-[R]		allosteric JNJ-27141491		allosteric SD-24
Radioligand - Construct	**pIC_{50} ± S.E.M. and (IC_{50} (nM))**								
^{125}I-CCL2 - CCR2	9.7 ± 0.2[a]	(0.21)	7.8 ± 0.2	(16)	6.1 ± 0.1	(746)	6.6 ± 0.1	(241)	< 5
^{125}I-CCL3 - CCR5	8.7 ± 0.4[b]	(1.9)	5.3 ± 0.2	(4508)	< 5		5.4 ± 0.1	(4254)	no displacement
^{125}I-CCL2 - CCR5-CCR2(all)	8.9 ± 0.3[a]	(1.3)	6.3 ± 0.1**	(516)	< 5		5.0 ± 0.1*	(10650)	no displacement
^{125}I-CCL3 - CCR5-CCR2(C-term)	8.9 ± 0.2[b]	(1.4)	no displacement		5.1 ± 0.1	(7638)	< 5		no displacement
^{125}I-CCL2 - CCR2-CCR5(C-term)	8.9 ± 0.2[a]	(1.4)	7.3 ± 0.1	(48)	5.7 ± 0.2	(1908)	6.4 ± 0.1	(364)	< 5

Data are presented as mean pIC_{50} ± S.E.M. and mean IC_{50} (nM) of at least three experiments performed in duplicate.
[a] pIC_{50} of CCL2.
[b] pIC_{50} of CCL3.
* p< 0.05 vs. CCR5, Student's *t*-test.
** p< 0.005 vs. CCR5, Student's *t*-test.

Table 2. IP turnover activation by chemokines and inhibition by small molecule antagonists for CCR2, CCR5 and the chimeric receptors expressed in COS-7 cells. In case of the assays with the antagonists, a chemokine concentration that evoked 80% of the maximum response (EC_{80}) was used. The chemokine that was used for each construct is indicated in the first column.

	endogenous ligands (CCL2 or CCL3)		orthosteric INCB3344		allosteric CCR2-RA-[R]		allosteric JNJ-27141491		allosteric SD-24	
Chemokine - Construct	**pEC_{50} ± S.E.M. and (EC_{50} (nM))**		**pIC_{50} ± S.E.M. and (IC_{50} (nM))**							
CCL2 - CCR2	9.2 ± 0.3	(0.63)	8.0 ± 0.01	(10)	7.0 ± 0.1	(93)	7.1 ± 0.1	(85)	6.6 ± 0.3	(236)
CCL3 - CCR5	8.1 ± 0.2	(8.0)	5.3 ± 0.01	(4645)	6.2 ± 0.1	(680)	5.9 ± 0.1	(1201)	5.3 ± 0.1	(5206)
CCL2 - CCR5-CCR2(all)	9.4 ± 0.3	(0.41)	7.0 ± 0.4*	(104)	5.2 ± 0.2**	(6227)	5.4 ± 0.2	(3837)	5.2 ± 0.1	(6133)
CCL3 - CCR5-CCR2(C-term)	8.1 ± 0.3	(7.4)	5.4 ± 0.1	(4399)	6.4 ± 0.1	(428)	5.6 ± 0.2	(2605)	5.6 ± 0.1*	(2301)
CCL2 - CCR2-CCR5(C-term)	9.3 ± 0.2	(0.48)	7.8 ± 0.2	(18)	6.9 ± 0.2	(126)	6.9 ± 0.1	(121)	6.4 ± 0.2	(388)

Data are presented as mean pEC_{50} ± S.E.M. and pIC_{50} ± S.E.M. as well as mean EC_{50} (nM) and mean IC_{50} (nM) of at least three experiments performed in duplicate.
* p < 0.05 vs. CCR5, Student's *t*-test.
** p < 0.005 vs. CCR5, Student's *t*-test.

The orthosteric antagonist INCB3344 displaced the radioligands ^{125}I-CCL2 and ^{125}I-CCL3 from CCR2 and CCR5, respectively, with a pIC_{50} of 7.8 ± 0.2 and 5.3 ± 0.2 (Table 1). Its pIC_{50} to inhibit IP turnover was 8.0 ± 0.01 for CCR2 and 5.3 ± 0.01 for CCR5 (Table 2). In comparison to the allosteric antagonists, INCB3344 showed a much lower affinity (280-fold) and potency (460-fold) for CCR5 compared to CCR2.

To better determine the affinity of INCB3344 and CCR2-RA-[R] for CCR2 and CCR5 we performed homologous displacement assays on membrane preparations of CHO cells transfected with CCR2 and CCR5. The pK_D of INCB3344 for CCR2 was 8.1 ± 0.1, whereas binding to CCR5 could not be detected at nanomolar concentrations of [^{3}H]-INCB3344. The pK_D of CCR2-RA-[R] for CCR2 and CCR5 was 8.8 ± 0.1 and 7.0 ± 0.1, respectively (Table 3). All these data together suggest that the orthosteric binding site is more divergent between CCR2 and CCR5 than the allosteric binding pocket.

Table 3. Displacement of [^{3}H]-INCB3344 binding and [^{3}H]-CCR2-RA binding from CHO membranes expressing FLAG-tagged CCR2, CCR5 and CCR2-CCR5(C-term) receptors.

	[^{3}H]-INCB3344	**[^{3}H]-CCR2-RA**
Construct	**pK_D ± S.E.M. and (K_D (nM))**	
CCR2	8.1 ± 0.1 (8.3)	8.8 ± 0.1 (1.7)
CCR5	no binding	7.0 ± 0.1 (100)
CCR2-CCR5(C-term)	8.6 ± 0.1 (2.3)	8.7 ± 0.1 (2.0)

Data are presented as mean pK_D ± S.E.M. or mean K_D (nM) of at least three experiments performed in duplicate.

CCR2-CCR5 chimeric approach. Given the high structural similarity between CCR2 and CCR5, we took CCR5 as a template structure to further elucidate the allosteric binding site in CCR2. Therefore we decided to use a chimeric approach to investigate the role of the extracellular loops and intracellular region of the receptor in binding of the antagonists (Fig. 3B). The chimera CCR5-CCR2(all), which consisted of CCR2's extracellular receptor regions, and CCR5 for the remainder of the construct, was used to study the role of the extracellular loops for small molecule binding. In order to study the role of the C-terminus in binding of the antagonists, two novel chimera's were constructed; CCR5-CCR2(C-term) and CCR2-CCR5(C-term), consisting of CCR5 with CCR2 C-terminus, and CCR2 with CCR5 C-terminus, respectively. We confined ourselves to the C-terminus, as the intracellular loops are highly similar in sequence between CCR2 and CCR5 (Fig. 3A).

For the two allosteric antagonists CCR2-RA-[R] and JNJ-27141491, the ability to inhibit binding of ^{125}I-CCL2 to CCR2 as well as the potency to inhibit IP3 formation by CCL2 was not affected when the C-terminal part of CCR5 was introduced in CCR2 (CCR2-CCR5(C-term)) (Tables 1 and 2). In addition, for CCR2-RA-[R] and JNJ-27141491 no difference was observed in their potency to inhibit IP3 formation by CCL3 between CCR5 and CCR5-CCR2(C-term) (Table 2). The displacement of ^{125}I-CCL3 from CCR5-CCR2(C-term) by CCR2-RA-[R], JNJ-27141491 and SD-24 could not be compared to CCR5, since their affinities were too low in a number of cases (Table 1). Similarly, SD-24 did not displace ^{125}I-CCL2 binding from CCR2 and CCR2-CCR5(C-term) (Table 1). However, the pIC_{50} value of SD-24 to inhibit IP3 formation via CCR5-CCR2(C-term) was with 5.6 ± 0.1 slightly higher than the pIC_{50} of 5.3 ± 0.1 for CCR5. All together, the data of the IP turnover assay suggest that non-conserved residues in the C-terminus of CCR2 compared to CCR5 are not involved in binding of the allosteric antagonists CCR2-RA-[R] and JNJ-27141491. For SD-24, a 2-fold increase in potency was observed upon introduction of the CCR2 C-terminus in CCR5, whereas introduction of the CCR5 C-terminus in CCR2 did not result in any changes.

Upon introduction of the extracellular loops of CCR2 in CCR5 (chimer CCR5-CCR2(all)), a significant decrease in potency to inhibit IP turnover was observed for CCR2-RA-[R] as its pIC_{50} value was 5.2 ± 0.2 for CCR5-CCR2(all) compared to 6.2 ± 0.1 in case of CCR5 (Table 2). In the binding assays the affinities of CCR2-RA-[R] and SD-24 for CCR5-CCR2(all) were negligible (Table 1). Differently, a slight decrease in affinity of JNJ-27141491 was observed, since its pIC_{50} value was 5.0 ± 0.1 for CCR5-CCR2(all) compared to 5.4 ± 0.1 for CCR5 (Table 1). It should be noted that we compared binding and activation of CCR5 by ^{125}I-CCL3/CCL3 with binding and activation of CCR5-CCR2(all) by ^{125}I-CCL2/CCL2. It can thus not be excluded that activation of these receptors in a molecularly different way could be responsible for the observations.

In contrast to the allosteric antagonists, the inhibitory potency and affinity of the orthosteric antagonist INCB3344 was increased for CCR5 when the extracellular loops of CCR2 were introduced. INCB3344 inhibited ^{125}I-CCL3 binding to CCR5 and ^{125}I-CCL2 binding to CCR5-CCR2(all) with a pIC_{50} of 5.3 ± 0.2 and 6.3 ± 0.1, respectively (Table 1). In addition, the potency of INCB3344 to inhibit CCL2-induced CCR5-CCR2(all) activity in the functional assay was increased 45-fold compared to its potency to inhibit CCL3-induced CCR5 activity (Table 2). Next we measured the effect of the C-terminus swap on the affinity and potency of INCB3344. For CCR2-CCR5(C-term) the affinity of INCB3344 and its potency to inhibit IP turnover were not significantly altered compared to CCR2. Exchange of the CCR5 C-terminus with that of CCR2 made INCB3344 unable to displace ^{125}I-CCL3 from CCR5-CCR2(C-term),

whereas the potency to inhibit IP turnover was similar for CCR5-CCR2(C-term) compared to CCR5.

The small molecule radioligands [^{3}H]-INCB3344 and [^{3}H]-CCR2-RA were only able to bind to CCR2-CCR5(C-term) of all three chimers, with a pK_D of 8.6 ± 0.1 and 8.7 ± 0.1, respectively (Table 3). Thus no significant change compared to the WT CCR2 pK_D of 8.8 ± 0.1 was observed for [^{3}H]-CCR2-RA, in agreement with the chemokine-displacement assays (Table 1 and 3). [^{3}H]-INCB3344 was found to bind slightly better to CCR2-CCR5(C-term) compared to CCR2 (pK_D = 8.1 ± 0.1), somewhat different than observed in the chemokine-displacement assays (Table 1 and 3).

Identification of intracellular residues involved in CCR2-RA-[R] binding. To further investigate the possibility of an intracellular binding pocket, we applied a site-directed mutagenesis approach. We initially constructed four mutations in CCR2, K72A$^{2.34}$, D78N$^{2.40}$, Y305A$^{7.53}$ and K311A$^{8.49}$ (Fig 3A+C). K72$^{2.34}$ in ICL1 is one of the few differential residues in the intracellular loops of CCR2 compared to CCR5 (Fig. 3A). Y305$^{7.53}$ is very conserved among G protein-coupled receptors, whereas D78$^{2.40}$ and K311$^{8.49}$ are typical residues among chemokine receptors (see also Discussion). As a control we included I208A$^{5.45}$, which was previously not predicted in any binding site, and E291A$^{7.39}$, which is the highly conserved acidic residue in the orthosteric binding pocket of chemokine receptors. All six mutant receptors were expressed at the cell surface, as determined by whole cell ELISA (Fig 4).

Mutation of Y305$^{7.53}$ into an alanine residue (Y305A) completely abolished [^{3}H]-CCR2-RA binding, whereas the affinity of [^{3}H]-INCB3344 was not affected (Table 4). The affinity of CCR2-RA-[R] for the K311A$^{8.49}$ mutant receptor was 10-fold decreased compared to WT CCR2, whereas the K72A$^{2.34}$ and D78N$^{2.40}$ mutations did not affect binding. The affinity of INCB3344 was not affected by any of these mutations at the intracellular region (Table 4). In contrast, the affinity of INCB3344 was 8-fold decreased for the E291A$^{7.39}$ mutant receptor compared to WT CCR2, whereas the affinity of CCR2-RA-[R] was not affected by this mutation located in the upper half of the receptor. These results reveal that the two residues Y305$^{7.53}$ and K311$^{8.49}$, both located at the transmembrane/intracellular side of the receptor, are involved in binding of the allosteric antagonist CCR2-RA-[R], whereas E291$^{7.39}$ in the orthosteric binding pocket is only important for binding of INCB3344 to CCR2.

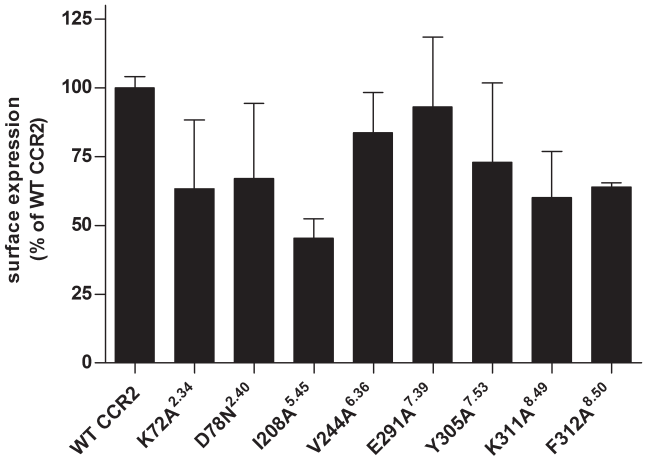

Fig. 4. Surface expression of the HA-tagged WT and mutant CCR2 receptors in CHO cells as measured by ELISA. Data was normalized for WT CCR2 expression (100%) and is presented as mean ± SD of at least two experiments performed in quadruplicate.

Table 4. Displacement of [^{3}H]-INCB3344 binding and [^{3}H]-CCR2-RA binding from CHO membranes expressing HA-tagged WT and mutant CCR2 receptors.

	[^{3}H]-INCB3344		[^{3}H]-CCR2-RA	
	displacement by INCB3344	displacement by CCR2-RA-[R]	displacement by JNJ-27141491	displacement by SD-24
Construct	pIC$_{50}$ ± S.E.M. and IC$_{50}$ (nM)			
WT CCR2	7.8 ± 0.03 (16)	7.8 ± 0.05 (16)	7.6 ± 0.1 (24)	7.8 ± 0.1 (16)
K72A$^{2.34}$	7.8 ± 0.01 (15)	7.7 ± 0.1 (21)	7.3 ± 0.1* (45)	7.6 ± 0.1 (24)
D78N$^{2.40}$	7.8 ± 0.1 (16)	7.7 ± 0.1 (21)	7.4 ± 0.1* (43)	7.5 ± 0.1* (33)
I208A$^{5.45}$	7.8 ± 0.1 (17)	7.7 ± 0.1 (19)	7.8 ± 0.1 (17)	7.9 ± 0.02 (12)
V244A$^{6.36}$	8.1 ± 0.03** (7.5)	no binding	ND	ND
E291A$^{7.39}$	6.9 ± 0.1** (126)	7.7 ± 0.1 (21)	7.7 ± 0.1 (22)	7.7 ± 0.05 (20)
Y305A$^{7.53}$	7.7 ± 0.03 (19)	no binding	ND	ND
K311A$^{8.49}$	7.7 ± 0.03 (18)	6.8 ± 0.1** (169)	7.5 ± 0.1 (30)	7.1 ± 0.1** (74)
F312A$^{8.50}$	8.0 ± 0.1** (9.2)	no binding	ND	ND

Data are presented as mean pIC$_{50}$ ± S.E.M. and mean IC$_{50}$ (nM) of at least three experiments performed in duplicate.
ND, not determined
* p< 0.05 vs. WT CCR2, Student's *t*-test.
** p< 0.005 vs. WT CCR2, Student's *t*-test.

Docking of CCR2-RA-[R] in a CCR2 homology model. To obtain further insight in the binding pose of CCR2-RA-[R], we constructed a CCR2 homology model using the crystal structure of CCR5 (PDB: 4MBS) and docked the antagonist CCR2-RA-[R] in the model. When standard docking was used, only low scoring poses were found. Therefore we employed induced-fit docking to account for the flexibility of the intracellular pocket. Final poses were selected based on both the score and consistency with experimental results. In Figure 5 the interactions of CCR2-RA-[R] with V244$^{6.36}$, K311$^{8.49}$, Y305$^{7.53}$ and F312$^{8.50}$ are visualized. The pocket is shielded by Y305$^{7.53}$ at the top and F312$^{8.50}$ at the side, both enabling hydrophobic interactions with CCR2-RA-[R]. K311$^{8.49}$ is turned towards the bottom of the binding pocket and interacts with one of the carbonyl oxygens in CCR2-RA-[R]. At the side of the binding pocket, V244$^{6.36}$ was found to interact with the hexyl-ring of CCR2-RA-[R]. The residues K72A$^{2.34}$ and D78$^{2.40}$ were not in close proximity to CCR2-RA-[R] (Fig. 5A), which was in agreement with their lack of effect on binding observed in the radioligand binding experiments (Table 4).

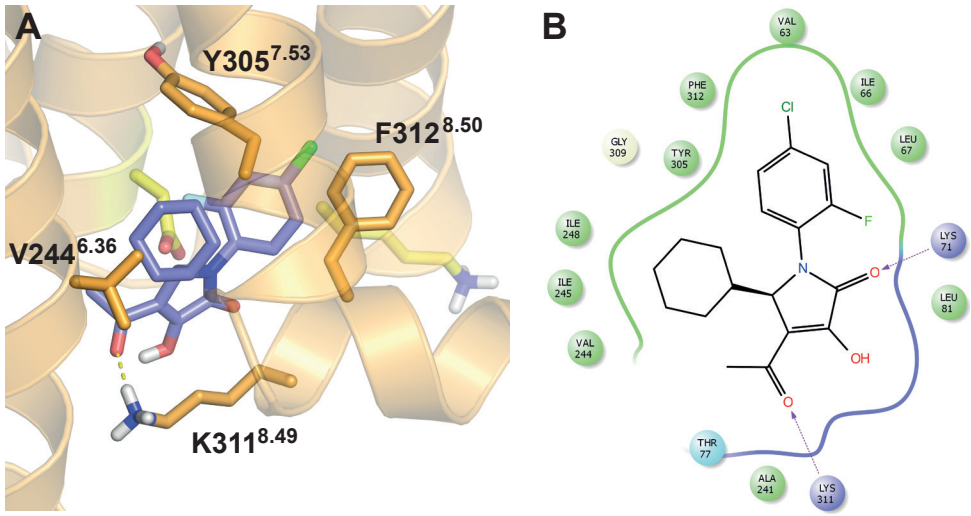

Fig. 5. (A) Induced fit docking of CCR2-RA-[R] in a homology model of CCR2 based on the crystal structure of CCR5. The pocket is shielded by Y305$^{7.53}$ at the top and F312$^{8.50}$ at the side, K311$^{8.49}$ is turned towards the bottom of the binding pocket and V244$^{6.36}$ interacts at the side with the hexyl-ring. D78$^{2.40}$ and K72$^{2.34}$ are represented in yellow, as these residues are not predicted to interact with CCR2-RA-[R]. (B) Interaction map of CCR2-RA-[R] with surrounding residues upon induced fit docking.

Experimental evidence for the docking pose of CCR2-RA-[R]. We determined the effect of mutagenesis of V244$^{6.36}$ in TM-VI and F312$^{8.50}$ in helix-VIII on binding of [^{3}H]-CCR2-RA, since these residues were predicted to be important for binding of CCR2-RA-[R] in the homology model. Both mutant receptors V244A$^{6.36}$ and F312A$^{8.50}$ were expressed at the cell surface, as

determined by whole cell ELISA (Fig. 4). Similar to Y305A$^{7.53}$, the binding of [^{3}H]-CCR2-RA was completely abolished for V244A$^{6.36}$ and F312A$^{8.50}$, while [^{3}H]-INCB3344 was able to bind with a slightly increased affinity to both mutant receptors in comparison to WT CCR2 (Table 4).

Binding site of JNJ-27141491 and SD-24. On the assumption that the small molecule antagonists JNJ-27141491 and SD-24 share the same binding site as CCR2-RA-[R], we subjected these two compounds to displacement studies with radiolabeled [^{3}H]-CCR2-RA on the series of CCR2 single point mutations (Table 4). JNJ-27141491 showed a small but significant affinity decrease in displacing [^{3}H]-CCR2-RA compared to wild-type CCR2 for the K72A$^{2.34}$ and D78N$^{2.40}$ mutant receptors of 1.8-fold in both cases. The affinity of SD-24 was 2-fold and 4.4-fold decreased for the D78N$^{2.40}$ and K311A$^{8.49}$ mutant receptors. Due to a lack of [^{3}H]-CCR2-RA binding to V244A$^{6.36}$, Y305A$^{7.53}$ and F312A$^{8.50}$, we could not use these mutants in the heterologous displacement assays. Neither I208A$^{5.45}$ nor E291A$^{7.39}$ affected the binding of the antagonists. These data confirm that JNJ-27141491 and SD-24 bind in the same region as CCR2-RA-[R], albeit with a different orientation, since K72$^{2.34}$, D78$^{2.40}$ and K311$^{8.49}$ differently affected the binding of the three allosteric antagonists. In agreement with these different binding poses, the best possible alignment of the three antagonists illustrated that these structures cannot be fully superimposed (Fig. 6). The substituted aromatic ring of CCR2-RA-[R] is overlaid with the aromatic ring structures of JNJ-27141491 and SD-24. However, at the position of the middle pyrroline ring structure of CCR2-RA-[R], SD-24 contains an aromatic ring whereas JNJ-27141491 extends further with its isoxazole ring.

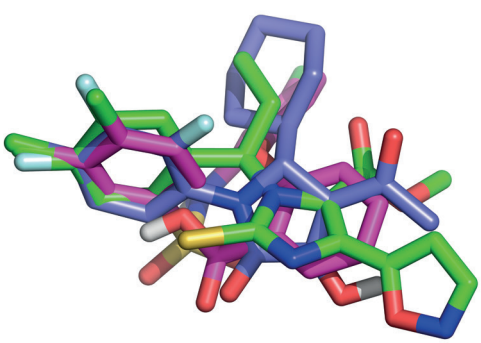

Fig. 6. Superimposition of CCR2-RA-[R] (lilac), JNJ-27141491 (green) and SD-24 (magenta). At the bottom right the different properties of the antagonists are illustrated: JNJ-27141491 is extended at this side with an isoxazole ring structure, and the aromatic ring structure of SD-24 is superimposed with the pyrroline ring structure of CCR2-RA-[R].

Effect of CCR2 mutations on receptor activation. The effects of the mutations on receptor activation were determined in a [^{35}S]GTPγS assay. [^{35}S]GTPγS binding was equal for mock transfected CHO cell membranes as for WT CCR2 CHO cell membranes (data not shown), and therefore no basal activity is reported in Figure 7. The mutations K72A$^{2.34}$, V244$^{6.36}$, E291A$^{7.39}$, Y305A$^{7.53}$, K311A$^{8.49}$ and F312A$^{8.50}$ distorted receptor activation as no [^{35}S]GTPγS binding window was observed upon addition of 100 nM CCL2 (Fig 5A). CCL2 was found to induce G protein-activation for WT CCR2 with a pEC$_{50}$ value of 7.6 ± 0.2 (Fig. 7B). D78N$^{2.40}$ was the only mutant receptor that allowed significant G protein-activation by CCL2, which yielded a pEC$_{50}$ value of 7.8 ± 0.1 (Fig. 7B).

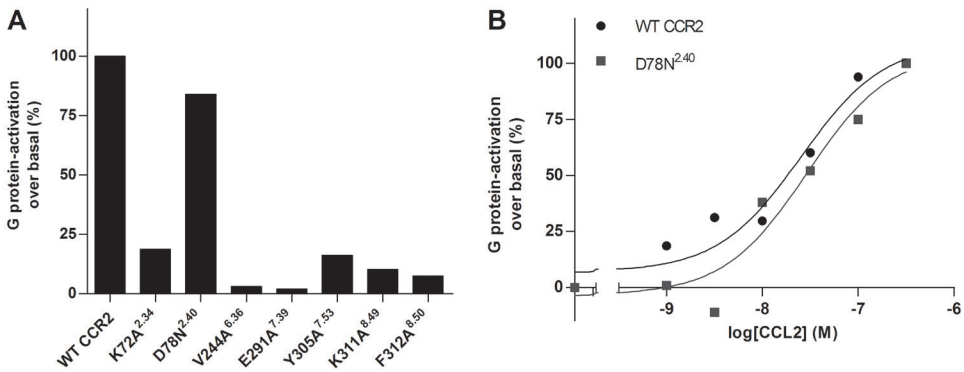

Fig. 7. (A) G protein-activation by CCL2 measured in a [^{35}S]GTPγS binding assay on CHO cell membranes expressing WT and mutant CCR2 receptors. (B) Concentration-effect curves of CCL2 on WT and D78N$^{2.40}$ CCR2 resulting in a pEC$_{50}$ of 7.6 ± 0.2 and 7.8 ± 0.1, respectively. A representative graph of one experiment performed in duplicate is shown.

Discussion

Since the early days of GPCR research, our understanding of ligands that activate or inhibit these receptors has increased dramatically [31, 32]. We can now distinguish GPCR ligands with a broad spectrum of activities and mechanisms of action, which implies the presence of multiple binding sites, including so-called allosteric binding sites [33]. In the present study we provided evidence for the presence of an allosteric intracellular binding site for small molecule antagonists of the chemokine receptor CCR2.

Without knowing their location on the receptor we have previously reported on multiple binding sites for small molecule CCR2 ligands, and classified CCR2-RA-[R] and JNJ-27141491 as allosteric antagonists based on radioligand binding studies [10]. Besides these, we now

identified SD-24 to bind at the same allosteric binding pocket at CCR2 (Fig. 2). Structurally related ligands with a pyrazinyl-sulfonamide scaffold have been reported to bind at the intracellular side of CCR4 [16]. Although the precise location of this binding site was not identified, interactions of these antagonists with the C-terminus of CCR4 were reported.

In order to elucidate the location of the CCR2 binding site for CCR2-RA-[R], JNJ-27141491 and SD-24, we constructed several CCR2-CCR5 chimeric receptors to identify regions responsible for binding. CCR2 and CCR5 bear a high sequence similarity of approximately 70%, which makes them perfect candidates for the construction of chimeric receptors [34, 35]. Besides the suggested intracellular binding site for CCR4, other allosteric ligands for chemokine receptors have been reported to interact with the extracellular loops (ECLs). ECL2 contributes to the CXCR4 binding site of the co-crystallized ligand It1 [15], and interactions with ECL2 were reported for the CCR5 antagonists AK530 [36], aplaviroc [20] and small molecule ligands targeting CCR1 and CCR8 [37].

We constructed CCR2-CCR5 chimeras in which either these extracellular regions or the C-terminus were swapped. Binding of the orthosteric CCR2 antagonist INCB3344 was not affected after exchange of the C-terminus in the chemokine-displacement assays, but the binding to CCR5 was increased when extracellular loops of CCR2 were introduced. This fits very well with an orthosteric binding mode, since other small molecule chemokine receptor ligands that bind to the major binding pocket have been found to also interact with ECL2 [20, 36, 37]. However, CCR5 binding of the allosteric antagonists CCR2-RA-[R], JNJ-27141491 and SD-24 was not improved after introduction of the ECLs of CCR2. The affinity and potency of CCR2-RA-[R] and JNJ-27141491 did not change after swapping the C-terminus between CCR2 and CCR5, while for SD-24 a small but significant increase in potency was measured upon introduction of the CCR2 C-terminus in CCR5. It should be noted that intracellular antagonists need to pass the cell membrane before they can exert receptor inhibition in case of the whole cell binding assays and functional assays. In these studies, the allosteric antagonists remarkably displayed up to 10-fold higher potency in the whole cell IP3 assay performed at 37 ºC compared to their IC_{50} in the whole cell binding assay performed at 4 ºC, whereas INCB3344 behaved similarly in both assays. In addition, the binding of the allosteric ligands to CCR2 in the whole cell assays at 4 ºC were much higher than the corresponding values in the membrane assays at 37 ºC (Table 1 and Fig. 2) [10]. Although different cellular systems were used in these distinct assays, the antagonist binding to the intracellular binding pocket could also explain the decreased affinities in whole cell assays at 4ºC due to putative difficulties to enter the cell at such a low temperature.

To explore the possibility of an intracellular binding site, we focused on three conserved residues among chemokine receptors that were previously reported to be involved in small molecule binding at CXCR2, being D78$^{2.40}$, Y305$^{7.53}$ and K311$^{8.49}$ [18]. The binding of [^{3}H]-CCR2-RA was completely abolished for Y305A$^{7.53}$, and a 10-fold decreased affinity was observed for K311A$^{8.49}$. Upon considering the important GPCR motifs in this intracellular region and subsequent induced fit docking in a CCR2 homology model we identified F312$^{8.50}$ and V244$^{6.36}$ as part of the intracellular pocket, and mutagenesis of these residues into alanine completely prevented [^{3}H]-CCR2-RA from binding. This data is in line with the unaffected affinity of the allosteric antagonists for the chimera's in which the C-terminus was swapped, since K$^{8.49}$ and F$^{8.50}$ are present in both CCR2 and CCR5.

Y305$^{7.53}$ is the highly conserved tyrosine in the NPxxY motif found in 92% of class A GPCRs and this motif has been shown to be important for receptor internalization, receptor signalling and activation [38-40]. For CCR2 we confirmed its critical role in signalling, since a loss of G protein-activation was observed for Y305A$^{7.53}$ (Fig. 7). The increasing number of GPCR crystal structures show that Y305$^{7.53}$ can interchange between multiple different states [41], which emphasizes the flexibility of this residue and therefore also its potential to contribute to the creation of an intracellular small molecule binding pocket.

Together with F312$^{8.50}$ which is conserved in 68% of class A GPCRs, Y305$^{7.53}$ forms the NPxxYx$_{5,6}$F motif [38]. The π-stacking interaction between F312$^{8.50}$ and Y305$^{7.53}$ directly links TM-VII and helix-VIII and keeps the receptor in an inactive state [40], as observed in multiple crystal structures including the recent CCR5 structure [42]. Upon activation, the aromatic stacking interaction is disrupted which allows Y305$^{7.53}$ to rotate into the helical TM core to permit receptor signalling [41]. In induced-fit docking with CCR2-RA-[R] we observed that Y305$^{7.53}$ likely shields the top of the binding pocket, whereas F312$^{8.50}$ is positioned between TM-VII and TM-I and may therefore contribute to hydrophobic interactions with the space-filling chlorine substituent on the phenyl ring of CCR2-RA-[R] (Fig. 5).

Besides Y305$^{7.53}$ and F312$^{8.50}$, the residues V244$^{6.36}$ and K311$^{8.49}$ were found important for binding of CCR2-RA-[R]. K311$^{8.49}$ is a basic, positively charged residue and therefore a likely partner to interact with the partially negative charge on the oxygen present in CCR2-RA-[R] (Fig. 1 and 5). This interaction was visualized in the docking pose, in which K311$^{8.49}$ was found to shield the bottom of the binding pocket. K$^{8.49}$ is highly conserved among chemokine receptors (68.4%), but otherwise not prevalent among class A GPCRs (5.7%). Besides in CCR2, this residue was also found to be important in CXCR2 for interaction with the acidic Pteridone-1, Sch527123 and SB265610 antagonists [17, 18]. It would be interesting to study whether such a basic residue at this position is facilitating the presence of a small molecule

binding pocket, in view of the prevalence of intracellular antagonists among the chemokine receptor family so far.

The loss of [^{3}H]-CCR2-RA binding upon the mutation of V244$^{6.36}$ into alanine confirms that TM-VI is involved in the creation of the intracellular small molecule binding pocket. Notably, it is TM-VI that moves outward on activation of GPCRs as has become evident from a comparison between active and inactive state crystal structures [43]. Besides steric hindrance by the antagonist for G protein binding, the fixation of TM-VI in an inactive state might be another mechanism by which these antagonists exert their inhibitory effect. Interestingly this valine residue is among the few differential intracellular residues between CCR2 and CCR5, since a leucine is present on this position in CCR5 (Fig. 3A). Clearly the presence of a valine is very important for high affinity binding of CCR2-RA-[R], and the extended alkyl chain of the leucine in CCR5 may cause steric hindrance preventing high affinity binding of CCR2-RA-[R].

JNJ-27141491 and SD-24 share the intracellular binding pocket of CCR2-RA-[R], but were found to interact differently with surrounding residues. K311A$^{8.49}$ showed a significant reduction in affinity for SD-24 (4-fold), whereas no change was observed for JNJ-27141491. A 2-fold change in affinity was observed for D78N$^{2.40}$ for both JNJ-27141491 and SD-24, and K72A$^{2.34}$ only affected JNJ-27141491. These two residues were not important for binding of CCR2-RA-[R], but do surround its binding pocket and therefore serve as likely interaction partners for structurally different antagonists like JNJ-27141491 and SD-24 (Fig. 5 and 6).

Importantly, the affinity of the orthosteric antagonist INCB3344 was not affected for any of the mutations at the intracellular interface. Instead a significantly reduced affinity of INCB3344 was observed for the E291A$^{7.39}$ mutation (8-fold), as was published before for other orthosteric antagonists [44, 45]. Of note, this is the first study with experimental data that confirms the interaction of INCB3344 with E291$^{7.39}$ of CCR2 – a residue that is known to function as an anchor point for many positively charged CC-chemokine receptor small molecules [9, 45]. Interestingly a slight increase in INCB3344 affinity was observed for the F312A$^{8.50}$ and V244A$^{6.36}$ mutant receptors. This could imply that these mutants induce an inactive conformation of the receptor, in agreement with their lack of G protein-activation in the [^{35}S]GTPγS assay, and thereby enhance binding of INCB3344.

Intracellular binding sites have become subject of study over the past few years. The cytoplasmic tails of CCR4, CCR5 and CXCR1 have been implicated in the binding of antagonists, as were several specific intracellular residues for antagonists of CXCR2, including equivalent residues we studied [16-18]. In addition, an allosteric modulator of the PAR1 receptor was found to act through helix-VIII [46]. In the current study we largely identified the location of this intracellular binding pocket for CCR2. Notably, we were for the first time able to visualize

such an intracellular binding pocket upon induced-fit docking of CCR2-RA-[R] in a CCR2 homology model that was constructed based on the recent crystal structure of CCR5 [42]. Previous attempts to predict the location of intracellular binding pockets in homology models most likely failed due to the lack of a closely related crystal structure [18].

In summary, the evidence for intracellular binding pockets at (chemokine) GPCRs is accumulating. The results of our mutagenesis and docking studies provide evidence for such an allosteric binding site on CCR2 at a defined location and may facilitate the design of novel intracellular antagonists for this and other chemokine receptors, and, hopefully, for GPCRs in general.

References

1. Jimenez, F., et al., *CCR2 plays a critical role in dendritic cell maturation: possible role of CCL2 and NF-kappa B.* J Immunol, 2010. 184(10): p. 5571-81.
2. Luster, A.D., *Chemokines--chemotactic cytokines that mediate inflammation.* N Engl J Med, 1998. 338(7): p. 436-45.
3. Fantuzzi, L., et al., *Loss of CCR2 expression and functional response to monocyte chemotactic protein (MCP-1) during the differentiation of human monocytes: role of secreted MCP-1 in the regulation of the chemotactic response.* Blood, 1999. 94(3): p. 875-83.
4. Mahad, D.J. and R.M. Ransohoff, *The role of MCP-1 (CCL2) and CCR2 in multiple sclerosis and experimental autoimmune encephalomyelitis (EAE).* Semin Immunol, 2003. 15(1): p. 23-32.
5. Quinones, M.P., et al., *The complex role of the chemokine receptor CCR2 in collagen-induced arthritis: implications for therapeutic targeting of CCR2 in rheumatoid arthritis.* J Mol Med (Berl), 2005. 83(9): p. 672-81.
6. Boring, L., et al., *Decreased lesion formation in CCR2-/- mice reveals a role for chemokines in the initiation of atherosclerosis.* Nature, 1998. 394(6696): p. 894-7.
7. White, F.A., S.K. Bhangoo, and R.J. Miller, *Chemokines: integrators of pain and inflammation.* Nat Rev Drug Discov, 2005. 4(10): p. 834-44.
8. Surgand, J.S., et al., *A chemogenomic analysis of the transmembrane binding cavity of human G-protein-coupled receptors.* Proteins, 2006. 62(2): p. 509-38.
9. Rosenkilde, M.M. and T.W. Schwartz, *GluVII:06--a highly conserved and selective anchor point for non-peptide ligands in chemokine receptors.* Curr Top Med Chem, 2006. 6(13): p. 1319-33.
10. Zweemer, A.J., et al., *Multiple Binding Sites for Small-Molecule Antagonists at the CC Chemokine Receptor 2.* Mol Pharmacol, 2013. 84(4): p. 551-61.
11. Shin, N., et al., *Pharmacological characterization of INCB3344, a small molecule antagonist of human CCR2.* Biochem Biophys Res Commun, 2009. 387(2): p. 251-5.
12. Scholten, D.J., et al., *Pharmacological modulation of chemokine receptor function.* Br J Pharmacol, 2011. 165(6): p. 1617-43.
13. Maeda, K., et al., *Structural and molecular interactions of CCR5 inhibitors with CCR5.* J Biol Chem, 2006. 281(18): p. 12688-98.
14. Rosenkilde, M.M., et al., *The minor binding pocket: a major player in 7TM receptor activation.* Trends Pharmacol Sci, 2010. 31(12): p. 567-74.
15. Wu, B., et al., *Structures of the CXCR4 chemokine GPCR with small-molecule and cyclic peptide antagonists.* Science, 2010. 330(6007): p. 1066-71.
16. Andrews, G., C. Jones, and K.A. Wreggett, *An intracellular allosteric site for a specific class of antagonists of the CC chemokine G protein-coupled receptors CCR4 and CCR5.* Mol Pharmacol, 2008. 73(3): p. 855-67.
17. Nicholls, D.J., et al., *Identification of a putative intracellular allosteric antagonist binding-site in the CXC chemokine receptors 1 and 2.* Mol Pharmacol, 2008. 74(5): p. 1193-202.
18. Salchow, K., et al., *A common intracellular allosteric binding site for antagonists of the CXCR2 receptor.* Br J Pharmacol, 2010. 159(7): p. 1429-39.
19. Peace, S., et al., *Identification of a sulfonamide series of CCR2 antagonists.* Bioorg Med Chem Lett, 2010. 20(13): p. 3961-4.
20. Thiele, S., et al., *Allosteric and orthosteric sites in CC chemokine receptor (CCR5), a chimeric receptor approach.* J Biol Chem, 2011. 286(43): p. 37543-54.
21. Ballesteros, J.A., Weinstein, H, *Integrated methods for the construction of three dimensional models and computational probing of structure-function relations in G-protein coupled receptors.* Methods Neurosci, 1995. 25: p. 366-428.

22. Kissow, H., et al., *Glucagon-like peptide-1 (GLP-1) receptor agonism or DPP-4 inhibition does not accelerate neoplasia in carcinogen treated mice.* Regul Pept, 2012. 179(1-3): p. 91-100.
23. Smith, P.K., et al., *Measurement of protein using bicinchoninic acid.* Anal Biochem, 1985. 150(1): p. 76-85.
24. Schrodinger, MacroModel, version 10.1, LLC, New York, NY, 2013.
25. Schrodinger, Prime, version 3.2, LLC, New York, NY, 2013.
26. Jacobson, M.P., et al., *A hierarchical approach to all-atom protein loop prediction.* Proteins, 2004. 55(2): p. 351-67.
27. Jacobson, M.P., et al., *On the role of the crystal environment in determining protein side-chain conformations.* J Mol Biol, 2002. 320(3): p. 597-608.
28. Sherman, W., H.S. Beard, and R. Farid, *Use of an induced fit receptor structure in virtual screening.* Chem Biol Drug Des, 2006. 67(1): p. 83-4.
29. Schrodinger, Schrodinger Suite 2013-2 Induced Fit docking protocol; Glide version 6.0, Schrodinger, LLC, New York, NY, 2013; Prime version 3.3, Schrodinger, LLC, New York, NY, 2013.
30. Schrodinger, The PyMOL Molecular Graphics System, Version 1.5.0.4 Schrodinger, LLC.
31. Furchgott, R.F., *Receptor mechanisms.* Annu Rev Pharmacol, 1964. 4: p. 21-50.
32. De Lean, A., J.M. Stadel, and R.J. Lefkowitz, *A ternary complex model explains the agonist-specific binding properties of the adenylate cyclase-coupled beta-adrenergic receptor.* J Biol Chem, 1980. 255(15): p. 7108-17.
33. Wootten, D., A. Christopoulos, and P.M. Sexton, *Emerging paradigms in GPCR allostery: implications for drug discovery.* Nat Rev Drug Discov, 2013. 12(8): p. 630-44.
34. Shields, D.C., *Gene conversion among chemokine receptors.* Gene, 2000. 246(1-2): p. 239-45.
35. Toda, E., et al., *FROUNT is a common regulator of CCR2 and CCR5 signaling to control directional migration.* J Immunol, 2009. 183(10): p. 6387-94.
36. Maeda, K., et al., *Involvement of the second extracellular loop and transmembrane residues of CCR5 in inhibitor binding and HIV-1 fusion: insights into the mechanism of allosteric inhibition.* J Mol Biol, 2008. 381(4): p. 956-74.
37. Jensen, P.C., et al., *Reversed binding of a small molecule ligand in homologous chemokine receptors - differential role of extracellular loop 2.* Br J Pharmacol, 2012. 166(1): p. 258-75.
38. Fritze, O., et al., *Role of the conserved NPxxY(x)5,6F motif in the rhodopsin ground state and during activation.* Proc Natl Acad Sci U S A, 2003. 100(5): p. 2290-5.
39. Kalatskaya, I., et al., *Mutation of tyrosine in the conserved NPXXY sequence leads to constitutive phosphorylation and internalization, but not signaling, of the human B2 bradykinin receptor.* J Biol Chem, 2004. 279(30): p. 31268-76.
40. Nygaard, R., et al., *Ligand binding and micro-switches in 7TM receptor structures.* Trends Pharmacol Sci, 2009. 30(5): p. 249-59.
41. Hulme, E.C., *GPCR activation: a mutagenic spotlight on crystal structures.* Trends Pharmacol Sci, 2013. 34(1): p. 67-84.
42. Tan, Q., et al., *Structure of the CCR5 chemokine receptor-HIV entry inhibitor maraviroc complex.* Science, 2013. 341(6152): p. 1387-90.
43. Kruse, A.C., et al., *Activation and allosteric modulation of a muscarinic acetylcholine receptor.* Nature, 2013. 504(7478): p. 101-6.
44. Hall, S.E., et al., *Elucidation of binding sites of dual antagonists in the human chemokine receptors CCR2 and CCR5.* Mol Pharmacol, 2009. 75(6): p. 1325-36.
45. Mirzadegan, T., et al., *Identification of the binding site for a novel class of CCR2b chemokine receptor antagonists: binding to a common chemokine receptor motif within the helical bundle.* J Biol Chem, 2000. 275(33): p. 25562-71.

46. Dowal, L., et al., *Identification of an antithrombotic allosteric modulator that acts through helix 8 of PAR1*. Proc Natl Acad Sci U S A, 2011. 108(7): p. 2951-6.

47. Brodmerkel, C.M., et al., *Discovery and pharmacological characterization of a novel rodent-active CCR2 antagonist*, INCB3344. J Immunol, 2005. 175(8): p. 5370-8.

48. Xue, C.B., et al., *3-Aminopyrrolidine derivatives as modulators of chemokine receptors*, 2004. Inventors, Incyte Corporation. PCT/US2003/037946.

49. Zou, D., et al., *Novel, acidic CCR2 receptor antagonists: from hit to lead*. Lett Drug Des Discov, 2007. 4: p. 185-191.

50. Doyon, J., et al., *Discovery of potent, orally bioavailable small-molecule inhibitors of the human CCR2 receptor*. Chem Med Chem, 2008. 3 (4): p. 660-9.